Published in final edited form as:
J Bone Miner Res. 2012 December ; 27(12): 2452–2463. doi:10.1002/jbmr.1701.

PKCδ Deficiency Perturbs Bone Homeostasis by Selective Uncoupling of Cathepsin K Secretion and Ruffled Border Formation in Osteoclasts

Viviana Cremasco[1,2], **Corinne E. Decker**[1], **Deborah Stumpo**[3], **Perry J. Blackshear**[3], **Keiichi I. Nakayama**[4], **Keiko Nakayama**[5], **Traian S. Lupu**[1], **Daniel B. Graham**[6,7], **Deborah V. Novack**[6], and **Roberta Faccio**[1,8]

[1]Department of Orthopaedics; Washington University School of Medicine; St. Louis, MO, 63110; USA

[3]Laboratory of Signal transduction; National Institute of Environmental Health Science; Research Triangle Park, NC, 27709; USA

[4]Department of Molecular and Cellular Biology; Medical Institute of Bioregulation; Kyushu University; Fukuoka, Fukuoka 812-8582; JAPAN

[5]Department of Developmental Genetics; Center for Translational and Advanced Animal Research; Graduate School of Medicine; Tohoku University; Aoba-ku, Sendai 980-8575; Japan

[6]Department of Pathology and Immunology; Washington University School of Medicine; St. Louis, MO, 63110; USA

Abstract

Bone homeostasis requires stringent regulation of osteoclasts, which secrete proteolytic enzymes to degrade the bone matrix. Despite recent progress in understanding how bone resorption occurs, the mechanisms regulating osteoclast secretion, and in particular the trafficking route of cathepsin K vesicles, remain elusive. Using a genetic approach, we describe the requirement for PKCδ in regulating bone resorption by affecting cathepsin K exocytosis. Importantly, PKCδ deficiency does not perturb formation of the ruffled border or trafficking of lysosomal vesicles containing the v-ATPase. Mechanistically, we find that cathepsin K exocytosis is controlled by PKCδ through modulation of the actin bundling protein MARCKS. The relevance of our finding is emphasized in vivo as PKCδ−/− mice exhibit increased bone mass and are protected from pathological bone loss in a model of experimental post-menopausal osteoporosis. Collectively, our data provide novel mechanistic insights into the pathways that selectively promote secretion of cathepsin K lysosomes independently of ruffled border formation, providing evidence for the presence of multiple mechanisms that regulate lysosomal exocytosis in osteoclasts.

Introduction

The lysosomal secretory apparatus represents an evolutionarily conserved mechanism that has been co-opted by many disparate cell types for specialized functions. Despite similarities with conventional lysosomes, secretory lysosomes are distinguished by their ability to fuse

[8]Correspondence should be addressed to: Roberta Faccio, Box 8233, 660 S. Euclid, St. Louis, MO 63110, USA, Phone: 314-747-4602, Fax: 314-362-0334, faccior@wustl.edu.
[2]Current address: Department of Cancer Immunology and AIDS, Dana Farber Cancer Institute; Boston, MA, 02115; USA.
[7]Current address: The Broad Institute of MIT and Harvard; Boston, MA, 02142; USA.

Disclosure
All the authors state that they have no conflicts of interest

with the plasma membrane and release their contents into the extracellular space (1). Recent progress in the field has characterized several of the steps dictating the trafficking route of secretory lysosomes. Distinct multisubunit tethering complexes have been described that direct secretory lysosome trafficking and facilitate vesicle fusion with the plasma membrane. However, to date it remains unclear whether a common molecular mechanism is operational for all secretory lysosomes or if unique pathways control exocytosis of distinct subsets of lysosomal vesicles.

Among several cell types that utilize the secretory lysosome machinery, osteoclasts are unique in their remarkable capacity to secrete proteases and hydrolases that degrade bone tissue, a process required for the maintenance of optimal bone mass (2–4). In order to resorb bone, the osteoclast must firmly adhere to the bone matrix through the αvβ3 integrin, which induces assembly of an actin ring structure that forms a sealing zone to isolate the bone matrix to be resorbed from the extracellular environment (5–8). As lysosomal vesicles fuse with the plasma membrane facing the bone (9), the accumulation of membrane forms a characteristic ruffled border, where the osteoclast secretory machinery converges (4). The electrogenic H+ ATPase (proton pump) and the Cl− channel ClC-7 are lysosomal membrane proteins delivered to the ruffled border for the production of HCl and subsequent dissolution of the inorganic bone matrix (10–12). In addition, several proteolytic enzymes are secreted through the ruffled border to degrade organic bone components. In particular, cathepsin K has been shown to be essential for bone resorption, given its capacity for degrading collagen, elastin and gelatin (13,14). Importantly, patients with loss of function mutations in the cathepsin K gene display pycnodysostosis, characterized by a pathological increase in bone mass (15,16).

To date, all of the genetic studies addressing the secretion process in osteoclasts have revealed that inhibition of secretion impairs formation of the ruffled border (17). In this context, deletion of the vesicular trafficking molecules Rab7, Rab3 or SytVII ablates the ruffled border (18–20). Thus, it remains unclear if secretion of lysosomal vesicles in the osteoclast occurs independently of ruffled border formation. Furthermore, Rab-mediated vesicular trafficking has been shown to modulate lysosomal secretion in other hematopoietic cells, such as T cells, neutrophils and mast cells (1). This has been interpreted as evidence of a single secretory pathway for lysosomal vesicles. Therefore, it is not known whether all the different pools of secretory lysosomes are delivered to the plasma membrane through common or separate mechanisms.

Spatial regulation of vesicle fusion with the plasma membrane has been shown to be regulated by diacylglycerol (DAG), an important second messenger generated by Phospholipases (21). In the osteoclast, DAG is generated by Phospholipase Cγ2 (PLCγ2). We have previously documented the importance of PLCγ2 in bone resorption (22), suggesting that DAG may control activation of the secretory machinery necessary to degrade bone. Among numerous DAG-responsive molecules, we now identify the serine/threonine kinase PKCδ as a downstream effector of PLCγ2 and a major regulator of cathepsin K secretion during bone resorption. Mechanistically, exocytosis of cathepsin K vesicles in osteoclasts is promoted by the DAG-PKCδ pathway through phosphorylation of the actin bundling protein MARCKS. Importantly, the pathway identified herein specifically modulates cathepsin K secretion independently of ruffled border formation or trafficking of the v-ATPase, suggesting the existence of multiple regulatory mechanisms for lysosomal secretion in osteoclasts.

Materials and Methods

Mice

PLCγ2−/− were kindly provided by Dr. JN Ihle (St. Jude Children's Research Hospital, Memphis, Tennessee, USA). PKCδ−/− and MARCKS−/− mice were previously described (23,24). All experiments were approved by the Washington University School of Medicine animal care and use committee.

Histology and μCT

Five-micron sections of fixed, decalcified, paraffin-embedded long bones were histochemically stained with TRAP to detect osteoclasts. For calcein labeling, non-decalcified, methacrylamide embedded-sections were analyzed with a Nikon Eclipse 80i microscope and a 2X objective. For μCT, 3D images from intact mouse femurs were obtained on a μCT40 scanner (Scanco Medical). For vital μCT, mice were anesthetized with Isoflurane and 100 sections below the growth plate of the tibia were analyzed using viva μCT40 scanner (Scanco Medical).

Surgical removal of ovaries

4 week-old female mice were anesthetized and underwent bilateral OVX via the dorsal approach, as previously described (25). Vital μCT was performed before removal of the ovaries and 4 weeks after.

Primary cell culture

Bone marrow derived macrophages were isolated from 6–8 week old mice as previously described (26). Briefly, the marrow space of mouse long bones was flushed with serum free Alpha medium (Sigma) and isolated cells were grown in the presence of 100ng/ml M-CSF for 3 days. Alternatively, fetal livers were isolated from day 13.5–14.5 embryos, and single cell suspensions were cultured in the presence of 100ng/ml M-CSF for 8 days to generate macrophages. To form osteoclasts, macrophages were cultured with 100ng/ml GST-RANKL and 10ng/ml M-CSF (osteoclastogenic medium) for 5 days, with medium replaced every 48 hrs.

Bone resorption

Bone marrow macrophages were cultured for 10 days on bovine bone slices at a concentration of 5×10^3 cells/ml in the presence of 10ng/ml M-CSF and 100ng/ml GST-RANKL. Cells were then removed from the bone surface using fresh PBS, and bone slices were stained with 20 μg/ml peroxidase-conjugated wheat-germ agglutinin(Sigma) for 30 min at room temperature, followed by incubation with 3,3′-diaminobenzidine (0.52 mg/ml in PBS containing 0.1% H_2O_2) for 30 min. Bone resorption pits were analyzed using a light microscope (Nikon) and quantified using Image J software. Culture supernatant was collected and analyzed for the presence of Collagen type I fragment using the CrossLaps ELISA (immunodiagnostic Systems) following the manufacturer's protocol.

Inorganic matrix resorption

10^5 bone marrow macrophages were cultured in osteoclastic medium for 4 days on hydroxyapatite coated osteologic slides (BD Biosciences, San Jose, CA). On the fourth day, slides were rinsed in pH7 water and treated with 5% sodium hypochlorite for 5 minutes. Analysis was performed using a bright field microscope without phase.

Cathepsin K secretion

Osteoclasts were grown in 24 well-plates (40.000 cells/well) for 5–7 days until confluent. Cells were stimulated by addition of 50 ng/ml of PMA or with 1 μM Latrunculin A (both from Sigma). For some experiments, bovine bone fines were collected during the generation of bone slices using a benchtop rotary saw (Butler scientific). Bone powder collected from the cutting was resuspended at a 1:1 ratio in alpha medium after extensive washings in ethanol. Cells were stimulated by addition of 100 μl of the same powder suspension. After indicated time points, supernatants were recovered and resolved on a SDS-page gel for the presence of cathepsin K. Cells were lysed as a total cell protein control.

Western blot and antibodies

Cells were lysed in RIPA buffer, resolved by SDS-page and subjected to western blot analysis. The following antibodies were used: anti- PKCδ, pPKCδ, pMARCKS, total ERK (Cell Signaling), anti-cathepsin K (Millipore) and anti-MARCKS (Santa Cruz). As secondary antibodies, either a goat anti-mouse (Thermo Scientific) or a donkey anti-rabbit (Santa Cruz) was utilized.

Plasmids, lentivirus generation

Short-hairpin RNA constructs targeting MARCKS were generated by the Genome Institute at Washington University. Two different combinations of shRNAs were utilized (MARCKS shRNA A: GCCAAGATAATATGCCACTAA + CTTCTCCTTCAAGAAGAG CAA; and MARCKS shRNA B: TCGTCGCCTTCCAAAGCAAAT + CTCCTCCACGTCG TCGCCCAA). As a negative control, a shRNA construct directed towards Luciferase was used (CACTCGGATATTTGATATGTG). All the shRNAs were cloned into pLKOpuro lentiviral vector, containing a puromycin resistance cassette for selection. To generate lentiviruses, 293 T cells were transfected with the silencing vectors, in combination with 8.2 and VSVg plasmids, using JetPEI and manufacturer's protocols (Polyplus transfection, Genesee Scientific). Viral supernatants were collected on day 2 and day 3 post-transfection and immediately used to infect freshly isolated bone marrow macrophages. After 24 hours, media containing selection (3μg/ml puromycin) was added to cells for 48 hours to select for transduced cells. To ensure silencing in mature cells, osteoclasts were grown in the presence of 1μg/ml puromycin. Efficiency of knockdown was evaluated using semi-quantitative RT-PCR.

Immunofluorescence and microscopy

Cells were fixed with 4% paraformaldehyde (Polysciences) for 10 minutes then rinsed 3 times with PBS. Primary antibody diluted in PBS supplemented with 3% BSA and 0.1% saponin was added for 2 hours at room temperature, followed by 2 hours incubation with secondary antibody together with FITC-phalloidin (Molecular Probes). The following antibodies were used: rat anti mouse CD107a (Lamp1, eBioscience), mouse monoclonal anti-cathepsin K, mouse monoclonal anti-MARCKS (Santa Cruz), anti mouse and anti rabbit 564 (both form Molecular Probes). The ABL-93 anti-Lamp2 antibody developed by JT August was obtained from the Developmental Studies Hybridoma Bank developed under the auspices of NICHD and maintained by the University of Iowa, Department of Biology, Iowa City, IA 52242. The antibody directed against the E subunit of the v-ATPase was a generous gift from Dr. Shannon Holliday (Department of Anatomy & Cell Biology, University of Florida College of Medicine, Gainesville, FL 32610) and Dr. Beth S. Lee (Department of Physiology and Cell Biology, The Ohio State University College of Medicine, Columbus, Ohio 43210). Slides were analyzed using a Nikon Eclipse 80i microscope and a 63X Plan APO objective. Images were captured with a Nikon DS-Qi1MC camera and analyzed using NIS-elements software (Nikon). Additionally, a Zeiss LSM510 Meta laser scanning

confocal microscope equipped with a 63X Plan APO objective was used, and orthogonal Z slices were acquired using Zeiss LSM510 software.

Transmission electron microscopy

Mature osteoclasts on bone chips were fixed in 2% paraformaldehyde/2.5% glutaraldehyde (Polysciences) in 100mM PIPES/0.5mM $MgCl_2$, for 1 hr at room temperature. Samples were washed in PBS and postfixed in 1% osmium tetroxide (Polysciences) for 1 hr. Samples were then rinsed extensively in dH_20 prior to staining with 1% aqueous uranyl acetate (Ted Pella) for 1 hr. Following several rinses in dH_20, samples were dehydrated in a graded series of ethanol and embedded in Eponate 12 resin (Ted Pella). Sections of 95 nm were cut with a Leica Ultracut UCT ultramicrotome, stained with uranyl acetate and lead citrate, and viewed on a JEOL 1200 EX transmission electron microscope.

Statistics

After validating normal distribution of data sets, two-tailed Student's *t* test was used for all comparisons, with a *P* value of <0.05 set as statistically significant.

Results

The DAG-effector PKCδ is required for lysosomal exocytosis of cathepsin K

Our lab has previously documented that osteoclast differentiation and function require PLCγ2, which catabolizes the conversion of PIP2 into PIP3 and DAG. Specifically, PLCγ2 governs osteoclast differentiation through IP3 production and NFATc1 induction. Overexpression of NFATc1 in PLCγ2−/− cells is sufficient to rescue osteoclast differentiation, but not bone resorption, suggesting that DAG may control the secretory machinery necessary to degrade bone. In this regard, C1 domain containing proteins are well characterized DAG-responsive molecules. Among C1-domain containing candidates, novel PKCs are recognized for the presence of a full C1 domain in their N-terminus, which binds to DAG facilitating plasma membrane localization and allosteric activation. Among four novel PKC paralogs, we found that PKCδ is highly expressed in osteoclasts (Figure S1). To assess whether PKCδ is activated downstream of PLCγ2, WT and PLCγ2−/− osteoclast precursors were plated onto the β3 integrin ligand vitronectin, and PKCδ phosphorylation at Thr 505 in the activation loop was assessed by western blot (Figure 1A). Activation of PKCδ occurred as early as 15 min upon adhesion and peaked at 30 min, and this event was dependent on PLCγ2, suggesting that PKCδ may be a DAG-effector downstream of PLCγ2 in resorbing osteoclasts.

Since DAG has been involved in vesicle fusion with the plasma membrane, we tested the hypothesis that PKCδ is required for secretion of lysosomal proteases, such as cathepsin K, responsible for bone resorption. For this purpose, we isolated WT and PKCδ−/− bone marrow macrophages and generated osteoclasts in vitro by culturing them with the osteoclastogenic cytokines M-CSF and RANKL for 7 days. Similar numbers of multinucleated mature cells and similar expression of osteoclastogenic genes was observed in WT and PKCδ−/− cultures (Figure S2), indicating that PKCδ-deficiency does not impair osteoclast differentiation.

Mature osteoclasts grown on bone slices were then stained for F-actin (to demarcate actin rings) and cathepsin K. As previously shown, in WT osteoclasts cathepsin K (in red) exclusively localized within the actin ring (in green), where secretion occurs (Figure 1B,C). On the contrary, in PKCδ−/− osteoclasts cathepsin K was dispersed throughout the cytoplasm, with a paucity of the enzyme inside actin rings (Figure 1B,C). By confocal microscopy we confirmed the presence of cathepsin K in the secretion zone representing the

ruffled border in WT cells (Figure 1D, xz and yz stacks). In contrast, in PKCδ−/− osteoclasts accumulation of the enzyme was visible in the cytoplasmic area near the ruffled border (Figure S3A) and, in line with this observation, presence of large intracellular vesicles was observed in PKCδ−/− cells by electron microscopy (Figure S3B). Consistently, cathepsin K was not properly secreted outside the ruffled border in PKCδ−/− osteoclasts (Figure 1D).

To further analyze the role of PKCδ in cathepsin K secretion we measured its release into the supernatant of osteoclast cultures stimulated with bone particles. As shown in Figure 1E, addition of bone particles to WT osteoclasts prompted the release of cathepsin K into the medium. In contrast, secretion of cathepsin K into the supernatant of PKCδ−/− cultures was dramatically reduced at all time points analyzed (Figure 1E). Moreover, addition of the DAG-analog PMA efficiently stimulated cathepsin K secretion in WT cells, but was less effective in PKCδ−/− osteoclasts (Figure 1F).

To assess the physiological relevance of this finding we analyzed the role of PKCδ in bone resorption. WT and PKCδ−/− cells were generated on bone slices in the presence of M-CSF and RANKL for 10 days, and areas of bone resorption (pits) were visualized using wheat-germ agglutinin. WT osteoclasts formed numerous and well defined pits (Figure 1G,H). In contrast, genetic disruption of PKCδ profoundly impaired osteoclast bone resorption, as documented by a significant decrease in the pit area (Figure 1G,H) and collagen type I fragment release into the medium (Figure 1I). These data support that DAG regulates cathepsin K secretion, and thus bone resorption, through the activation of PKCδ.

PKCδ deficiency does not impair ruffled border formation or trafficking of lysosomes containing the v-ATPase

Fusion of secretory lysosomes with the plasma membrane region contained within the actin ring is required for formation of the ruffled border, comprised of highly convoluted membrane structures juxtaposed to the bone matrix where resorption occurs. Based on our findings illustrating the requirement for PKCδ in mediating secretion of cathepsin K lysosomes, we expected ruffled border formation to be impaired in the absence of PKCδ. Surprisingly, electron-microscopic analysis of PKCδ−/− osteoclasts plated on bone slices revealed that PKCδ−/− cells displayed well defined ruffled borders (Figure 2A, RB). To further address if PKCδ controls targeting of other lysosomal vesicles to the ruffled border, we analyzed the localization of the vacuolar-ATPase (v-ATPase), also known as the proton pump, and of the integral lysosomal membrane proteins Lamp1 and Lamp2. Confocal images showed that these lysosomal proteins localized in the ruffled border of both of WT and PKCδ−/− osteoclasts (Figure 2B, in red). Consistent with efficient delivery of the v-ATPase to the ruffled border, PKCδ−/− and WT osteoclasts equally dissolved hydroxyapatite coated slides, which occurs exclusively through release of protons and acidification of the resorptive lacuna (Figure 2C and quantified in Figure 2D). Thus, PKCδ-deficiency selectively impairs cathepsin K lysosome exocytosis without affecting trafficking of other lysosome-derived vesicles, supporting the existence of discrete pathways regulating secretion of lysosomal vesicles.

PKCδ controls bone homeostasis in physiological and pathological conditions

In order to determine the biological consequences of a selective impairment in cathepsin K lysosome exocytosis, we analyzed the bone phenotype of PKCδ−/− mice in vivo. Towards this end, 8 week old sex-matched WT and PKCδ−/− mice were sacrificed, and long bones were subjected to μCT analysis. PKCδ−/− mice exhibited significantly increased trabecular bone compared to their WT littermates, as determined by μCT examination and as shown in 3D-reconstructed images (Figure 3A). The percentage of trabecular bone volume versus

total volume was nearly doubled in PKCδ−/− mice compared to WT, with increased trabecular number and reduced trabecular space. (Figure 3B). TRAP staining of histological sections from tibias of WT or null animals revealed that osteoclast numbers were preserved in the absence of PKCδ, mirroring the in vitro observations (Figure 3C). Moreover, no increased osteoblast activity was observed in age-matched mice (Figure S4), indicating that the elevated bone mass in PKCδ−/− mice is due to defective bone resorption rather than increased bone formation. To determine the contribution of PKCδ in regulating bone mass in pathological bone loss, age-matched WT and PKCδ−/− female mice were subjected to ovariectomy, a condition that simulates post-menopausal osteoporosis due to enhanced osteoclast bone resorption. Trabecular bone volume was analyzed using vital μCT analysis before and 1 month after ovary removal. After ovariectomy, the percentage of trabecular bone volume remained significantly higher in PKCδ−/− mice, as compared to their WT littermates. In fact, while WT animal lost about 30% of their initial trabecular bone, PKCδ−/− mice were protected from bone loss (Figure 3D,E). These data demonstrate that selective blockade of cathepsin K secretion by PKCδ ablation has important consequences on physiological and pathological bone homeostasis.

MARCKS attenuates cathepsin K lysosomal secretion downstream of PKCδ

We then sought to determine the mechanisms by which PKCδ promotes cathepsin K secretion and bone resorption. Given that the ruffled border is an actin rich structure (27), we hypothesized that PKCδ might control release of cathepsin K through modulation of a target molecule with actin binding properties. Thus, we focused on Myristoylated Alanine-Rich C-Kinase Substrate (MARCKS), a substrate of PKCδ which in itsnon-phosphorylated form has been shown to have greater actin binding affinity, while in its phosphorylated form releases actin filaments from the plasma membrane (28). Notably, we found that MARCKS localizes in the ruffled border, (Figure 4A), while we did not observe its presence in the actin ring. Furthermore, we found that MARCKS is phosphorylated in osteoclasts upon adhesion, and its phosphorylation requires PKCδ (Figure 4B). Consistent with a role for DAG-dependent PKCδ activation, PLCγ2 is also required for MARCKS phosphorylation (Figure S5).

To determine the role of MARCKS in the regulation of lysosomal vesicle secretion, and thus bone resorption, we analyzed MARCKS−/− osteoclasts. In the absence of MARCKS, we predicted that filamentous actin within the ruffled border would be destabilized. Although MARCKS deficiency in mice is lethal due to aberrant neuronal development (23), KO embryos survive until day 14–15, when hematopoietic cells are abundant in the liver. Thus, we generated MARCKS−/− osteoclasts by culturing fetal liver cells in the presence of M-CSF and RANKL. We observed no impairment in osteoclast differentiation in MARCKS−/− cultures, either on plastic or on bone slices (Figure S6). Furthermore, MARCKS deficiency did not impair ruffled border formation, as localization of the proton pump in the ruffled border was not altered in MARCKS −/− osteoclasts (Figure S6). Strikingly, we found that MARCKS−/− osteoclasts showed increased release of cathepsin K, as measured by western blot analysis of supernatants from osteoclast cultures stimulated with bone particles (Figure 4C). As further evidence of enhanced cathepsin K secretion, MARCKS−/− osteoclasts exhibited excessive bone resorption capacity, generating more numerous resorptive pits compared to WT osteoclasts (Figure 4D,E). Similarly, release of collagen type I into the medium was increased in cultures from MARCKS−/− cells (Figure 4F). These data suggest a model in which MARCKS stabilizes actin filaments in the ruffled border, thus creating a barrier to secretion that must be physically removed to accommodate fusion of cathepsin K vesicles with the plasma membrane. In support of this model, treatment of osteoclasts with Latrunculin A, which inhibits actin polymerization (29) and thus induces filament destabilization, was sufficient to promote robust cathepsin K release (Figure 4G).

MARCKS silencing in PKCδ−/− osteoclasts restores cathepsin K vesicle exocytosis

MARCKS couples filamentous actin to the plasma membrane only in its non-phosphorylated state (30). Thus, it is conceivable that accumulation of non-phosphorylated MARCKS at the ruffled border of PKCδ−/− osteoclasts may stabilize actin filaments to form a barrier that prevents cathepsin K release. In this instance, it could be postulated that defective cathepsin K secretion in PKCδ−/− osteoclasts would be restored by MARCKS depletion. In order to test this hypothesis we silenced MARCKS in PKCδ−/− cells. Two MARCKS shRNAs were transduced into PKCδ−/− osteoclasts, which gave similar knock-down efficiencies (Figure 5A). A silencing construct targeting luciferase was used as a negative control. Transduced cells were differentiated into mature osteoclasts and stimulated with bone particles for 1, 3 or 16 hours, prior to analysis of cathepsin K secretion by western blot of culture supernatants. Consistent with our findings in MARCKS−/− cells, secretion was enhanced in WT osteoclasts transduced with either MARCKS shRNA, as compared to the luciferase control (Figure 5B). More importantly, silencing of MARCKS in PKCδ−/− cells was sufficient to restore secretion of cathepsin K (Figure 5B). Consistently, we found that MARCKS silencing augmented resorptive pit formation in WT cells and rescued bone resorption in PKCδ−/− osteoclasts (Figure 5C,D). Thus, MARCKS is the PKCδ effector modulating cathepsin K secretion and bone resorption in osteoclasts.

Taken together, our data identify the PKCδ-MARCKS pathway as a novel signaling module controlling cathepsin K secretion in osteoclasts. Importantly, we provide compelling evidence demonstrating the existence of discrete secretory pathways in osteoclasts, suggesting that trafficking of secretory lysosomes is achieved by multiple mechanisms within the same cell.

Discussion

The present study provides an important contribution to the understanding of lysosome secretion in osteoclasts, identifying the DAG-PKCδ pathway as a novel regulator of discrete pools of lysosomes during bone resorption. In light of the lysosomal origin of cathepsin K containing vesicles, it was previously assumed that the mechanisms regulating secretion of cathepsin K fundamentally overlap with those required for ruffled border formation, which is also controlled by lysosomal vesicular trafficking (17). We now find that PKCδ deficiency mediates cathepsin K secretion, without perturbing formation of the ruffled border. Thus, our study challenges the previous model and implies that secretion of bone degrading enzymes and formation of the ruffled border may be differentially regulated in osteoclasts. Indeed, we found that translocation of vesicles containing the vacuolar-ATPase to the ruffled border is unperturbed in absence of PKCδ and thus PKCδ−/− osteoclasts are not impaired in their ability to dissolve the inorganic bone matrix. Although the v-ATPase vesicles are also of lysosomal origin, the finding that PKCδ is preferentially involved in cathepsin K secretion suggests that vesicle cargo may determine how the lysosomal vesicles are delivered to the plasma membrane for exocytosis. Consistent with this concept, a recent study reported that disruption of the Man-6-P pathway in osteoclasts enhanced cathepsin K vesicle secretion without affecting trafficking of cathepsin D (31). This finding, along with our data, demonstrates the existence of different pools of secretory lysosomes in osteoclasts, each relying on a unique machinery essential for exocytosis. Whether or not other cells containing secretory lysosomes, such as T cells, neutrophils and mast cells, utilize similar mechanisms to specifically mobilize discrete pools of lysosomes for exocytosis, requires further investigation. Such flexibility would allow cells to secrete specialized lysosomal cargo in an appropriate context-specific manner.

The in vivo relevance of our findings highlights that selective disruption of cathepsin K lysosome secretion in osteoclasts by targeting of PKCδ has important implications on bone

health in vivo. In fact, PKCδ−/− animals display a significant increase in bone mass in basal conditions. Moreover, PKCδ deficiency protects animals from experimental postmenopausal osteoporosis, indicating that PKCδ might be a candidate target to prevent pathological bone loss. Notably, a previous report showed that PKCδ homozygous mutant mice exhibit defective embryonic bone formation, due to impaired osteoblast maturation (32). Nevertheless, PKCδ−/− mice are born without obvious bone morphogenic defects and osteoblast activity does not appear to be affected by PKCδ deficiency in adult mice. On the contrary, defective osteoclast function accounts for the increased bone mass observed in PKCδ−/− mice, suggesting that the opposite phenotypes between pre- and post-natal life in PKCδ−/− animals depends on a differential requirement for PKCδ in osteoblasts versus osteoclasts during ontogeny. While during embryonic bone formation PKCδ is required for osteoblast maturation, after birth PKCδ is required for osteoclasts to resorb the pre-existing bone matrix.

Activation of PKCδ in osteoclasts is contingent upon DAG production by Phospholipases. We have previously documented the importance of PLCγ2 signaling in osteoclasts in vitro and in vivo. Specifically we found that PLCγ2-dependent calcium fluxes controls osteoclast formation but not function, suggesting that PLCγ2-mediated DAG production is required for bone resorption (22,23). Due to lack of specific tools to modulate local DAG levels, it has been very difficult to understand the role of DAG in osteoclast functions. For instance, earlier studies using DAG mimetics have shown inhibition of pit formation, suggesting that DAG was a negative regulator of bone resorption (33). However, since spatial and temporal DAG production is tightly regulated, the use of DAG mimetics, especially for longer period of time, may not reflect the real effect of DAG-mediated signaling in the cell. We now show that treatment of osteoclasts with the DAG-analog PMA for short periods of time stimulates cathepsin K secretion. This finding is consistent with other studies utilizing DAG-mimetics indicating that an increase in DAG production potentiates secretion in a variety of cells (34,35). Furthermore, we provide genetic evidence that reduction in DAG production via PLCγ2 deficiency or ablation of the DAG-effector PKCδ, impairs cathepsin K secretion, thus positioning DAG-mediated pathways as an important target for anti-resorptive therapies.

Mechanistically, our study demonstrates that MARCKS is the PKCδ substrate regulating cathepsin K secretion and bone resorption. MARCKS contains actin binding sites that enable the binding and cross-linking of actin filaments (30,36,37). In steady state conditions, MARCKS is un-phosphorylated and associates with membranes via a myristic acid moiety and electrostatic interactions with phospholipids. Functionally, un-phosphorylated MARCKS anchors the actin cytoskeleton to the membrane (30). Phosphorylation of MARCKS introduces negative charges into the effector domain, thus interfering with its binding to the plasma membrane and affinity for actin (36,37). Consequently, MARCKS phosphorylation leads to local detachment of actin filaments from the membrane (38,39). In the osteoclast, we find that MARCKS is present in the ruffled border, and it is phosphorylated by PKCδ during adhesion. More importantly, MARCKS deletion in osteoclasts enhances bone resorption and its silencing in PKCδ−/− cells rescues their resorptive ability.

The data presented herein suggest a model in which non-phosphorylated MARCKS bundles actin filaments to the plasma membrane within the ruffled border, creating an actin barrier that prevents cathepsin K vesicles from being secreted (Figure 6). PKCδ-mediated MARCKS phosphorylation relieves MARCKS of its actin-membrane anchoring function, thus promoting local actin disruption. Free from the physical actin barrier, cathepsin K vesicles can fuse with the plasma membrane to release their contents into the extracellular matrix (Figure 6A). PKCδ-deficiency compromises phosphorylation of MARCKS and

removal of the actin barrier, thus limiting cathepsin K secretion (Figure 6B). In line with this model, we found greater accumulation of cathepsin K in the cytoplasm of PKCδ−/− osteoclasts in proximity of the ruffled border. A similar phenomenon has been observed in chromaffin cells, in which phosphorylation of MARCKS is necessary for actin disassembly at the plasma membrane and secretion of adrenaline-filled vesicles (40–42). Furthermore, there is evidence that remodeling of actin might be required for vesicle secretion in pancreatic beta cells and mast cells (35,43). More recently, Brown et al. extended this concept to NK cells, where it was reported that lytic granules are specifically secreted in areas of active cortical actin remodeling (44). Consistent with these reports, actin depolymerization by treatment of osteoclasts with Latrunculin A promoted cathepsin K secretion.

Based on our model, it remains uncertain why the presence of an actin barrier in PKCδ−/− osteoclasts does not affect formation of the ruffled border or translocation to the ruffled border of vesicles containing the v-ATPase. At least three possibilities are plausible. First, vesicle size could affect their ability to pass through the actin mesh that constitutes the barrier. Second, formation of the ruffled border by fusion of vesicles containing the v-ATPase (PKCδ-independent), and secretion of cathepsin K (PKCδ-dependent) may occur sequentially. In this context, cathepsin K secretion might be exquisitely sensitive to the presence of an actin barrier because these vesicles must be continuously released to sustain bone resorption. Last, an intriguing possibility is that different pools of vesicles are conveyed to specific docking sites in the ruffled border. Whether the exocytotic process in osteoclasts is differentially regulated based on the type of vesicles to be secreted, or whether spatial-temporal sequestration of docking sites dictates the specificity of secretion, requires further investigation.

In conclusion, the data we present demonstrate the requirement for DAG-PKCδ pathway regulating cathepsin K exocytosis, independent of ruffled border formation. Perhaps more importantly, our findings provide compelling evidence for the existence of multiple secretory pathways controlling lysosomal vesicular trafficking in osteoclasts. Thus, inhibition of PKCδ may represent an attractive therapeutic opportunity to selectively target secretion of cathepsin K during pathological bone loss.

Supplementary Material

Refer to Web version on PubMed Central for supplementary material.

Acknowledgments

We gratefully thank Dr. Steven Teitelbaum (Department of Pathology and Immunology, Washington University) for helpful discussion, Dr. Wei Zou (Department of Pathology and Immunology, Washington University) for his help with the ovariectomy surgical procedure and Dr. Wandy L. Beatty (Molecular Microbiology Imaging Facility, Washington University) for electron-microscopy.

This work was supported by National Institute of Health Grant 5R01 AR053628 to RF, Shriners Hospital Grant 85120 to RF, Arthritis Foundation Grant to RF, American Heart Association Grant 10PRE4030030 to VC, and NIH grants AR052705 and EB007568 to DVN. The study was supported in part by the Intramural Research Program of the NIH, NIEHS (PJB). The histological and μCT analysis were supported by The Center for Musculoskeletal Biology and Medicine at Washington University, Award Number P30AR057235 from the National Institute of Arthritis, Musculoskeletal and Skin Diseases. The silencing constructs were provided by the Genome Center at Washington University, Grant number CDI-LI-2010-94 from the Children's Discovery Institute to S. Stewart, E. Mardis and D. Piwnica-Worms.

Author's role: VC designed and performed the experiments and wrote the paper; CED performed some of the experiments; DS and PJB generated the MARCKS−/− mice; NIK and NK generated the PKCδ−/− mice; TSL helped with the in vivo experiments; DBG and DVN helped designing the experiments and writing the paper; RF designed the experiments and wrote the paper. VC and RF take responsibility for the integrity of the data analysis.

References

1. Blott EJ, Griffiths GM. Secretory lysosomes. Nat Rev Mol Cell Biol. 2002; 3(2):122–31. [PubMed: 11836514]
2. Novack DV, Teitelbaum SL. The osteoclast: friend or foe? Annu Rev Pathol. 2008; 3:457–84. [PubMed: 18039135]
3. Zaidi M. Skeletal remodeling in health and disease. Nat Med. 2007; 13(7):791–801. [PubMed: 17618270]
4. Teitelbaum SL, Ross FP. Genetic regulation of osteoclast development and function. Nature Reviews Genetics. 2003; 4:638–649.
5. Collin O, Tracqui P, Stephanou A, Usson Y, Clement-Lacroix J, Planus E. Spatiotemporal dynamics of actin-rich adhesion microdomains: influence of substrate flexibility. J Cell Sci. 2006; 119(Pt 9): 1914–25. [PubMed: 16636076]
6. Teti A, Grano M, Carano A, Colucci S, Zambonin Zallone A. Immunolocalization of beta 3 subunit of integrins in osteoclast membrane. Boll Soc Ital Biol Sper. 1989; 65 (11):1031–7. [PubMed: 2629822]
7. Vaananen HK, Horton M. The osteoclast clear zone is a specialized cell-extracellular matrix adhesion structure. Journal of Cell Science. 1995; 108:2729–2732. [PubMed: 7593313]
8. Nakamura I, Pilkington MF, Lakkakorpi PT, Lipfert L, Sims SM, Dixon SJ, Rodan GA, Duong LT. Role of avb3 integrin in osteoclast migration and formation of the sealing zone. Journal of Cell Science. 1999; 112:3985–3993. [PubMed: 10547359]
9. Baron R, Neff L, Brown W, Courtoy PJ, Louvard D, Farquhar M. Polarized secretion of lysosomal enzymes: Co-distribution of cation-independent mannose-6-phosphate receptors and lysosomal enzymes along the osteoclast exocytic pathway. Journal of Cell Biology. 1988; 106:1863–1872. [PubMed: 2968345]
10. Palokangas H, Mulari M, Vaananen HK. Endocytic pathway from the basal plasma membrane to the ruffled border membrane in bone-resorbing osteoclasts. Journal of Cell Science. 1997; 110(Pt 15):1767–1780. [PubMed: 9264464]
11. Vaananen HK, Karhukorpi EK, Sundquist K, Wallmark B, Roininen I, Hentunen T, Tuukkanen J, Lakkakorpi P. Evidence for the presence of a proton pump of the vacuolar H(+)-ATPase type in the ruffled borders of osteoclasts. J Cell Biol. 1990; 111(3):1305–11. [PubMed: 2144003]
12. Baron R, Neff L, Louvard D, Courtoy PJ. Cell-mediated extracellular acidification and bone resorption: evidence for a low pH in resorbing lacunae and localization of a 100-kD lysosomal membrane protein at the osteoclast ruffled border. J Cell Biol. 1985; 101(6):2210–22. [PubMed: 3905822]
13. Gowen M, Lazner F, Dodds R, Kapadia R, Feild J, Tavaria M, Bertoncello I, Drake F, Zavarselk S, Tellis I, Hertzog P, Debouck C, Kola I. Cathepsin K knockout mice develop osteopetrosis due to a deficit in matrix degradation but not demineralization. Journal of Bone & Mineral Research. 1999; 14(10):1654–1663. [PubMed: 10491212]
14. Drake FH, Dodds RA, James IE, Connor JR, Debouck C, Richardson S, Leerykaczewski E, Coleman L, Rieman D, Barthlow R, Hastings G, Gowen M. Cathepsin K, but not Cathepsins B, L, or S, is abundantly expressed in human osteoclasts. Journal of Biological Chemistry. 1996; 271:12511–12516. [PubMed: 8647859]
15. Johnson MR, Polymeropoulos MH, Vos HL, Ortiz de Luna RI, Francomano CA. A nonsense mutation in the cathepsin K gene observed in a family with pycnodysostosis. Genome Res. 1996; 6(11):1050–5. [PubMed: 8938428]
16. Gelb BD, Shi GP, Chapman HA, Desnick RJ. Pycnodysostosis, a lysosomal disease caused by cathepsin K deficiency. Science. 1996; 273:1236–1238. [PubMed: 8703060]
17. Stenbeck G. Formation and function of the ruffled border in osteoclasts. Semin Cell Dev Biol. 2002; 13(4):285–92. [PubMed: 12243728]
18. Zhao H, Ettala O, Vaananen HK. Intracellular membrane trafficking pathways in bone-resorbing osteoclasts revealed by cloning and subcellular localization studies of small GTP-binding rab proteins. Biochem Biophys Res Commun. 2002; 293:1060–1065. [PubMed: 12051767]

19. Zhao H, Laitala-Leinonen T, Parikka V, Vaananen HK. Downregulation of Small GTPase Rab7 Impairs Osteoclast Polarization and Bone Resorption. J Biol Chem. 2001; 276(42):39295–39302. [PubMed: 11514537]
20. Zhao H, Ito Y, Chappel J, Andrews NW, Teitelbaum SL, Ross FP. Synaptotagmin VII regulates bone remodeling by modulating osteoclast and osteoblast secretion. Dev Cell. 2008; 14(6):914–25. [PubMed: 18539119]
21. Dumas F, Byrne RD, Vincent B, Hobday TM, Poccia DL, Larijani B. Spatial regulation of membrane fusion controlled by modification of phosphoinositides. PLoS One. 2010; 5(8):e12208. [PubMed: 20808914]
22. Epple H, Cremasco V, Zhang K, Mao D, Longmore GD, Faccio R. Phospholipase Cgamma2 modulates integrin signaling in the osteoclast by affecting the localization and activation of Src kinase. Mol Cell Biol. 2008; 28(11):3610–22. [PubMed: 18378693]
23. Stumpo DJ, Bock CB, Tuttle JS, Blackshear PJ. MARCKS deficiency in mice leads to abnormal brain development and perinatal death. Proc Natl Acad Sci U S A. 1995; 92(4):944–8. [PubMed: 7862670]
24. Miyamoto A, Nakayama K, Imaki H, Hirose S, Jiang Y, Abe M, Tsukiyama T, Nagahama H, Ohno S, Hatakeyama S, Nakayama KI. Increased proliferation of B cells and auto-immunity in mice lacking protein kinase Cdelta. Nature. 2002; 416(6883):865–9. [PubMed: 11976687]
25. Ito Y, Teitelbaum SL, Zou W, Zheng Y, Johnson JF, Chappel J, Ross FP, Zhao H. Cdc42 regulates bone modeling and remodeling in mice by modulating RANKL/M-CSF signaling and osteoclast polarization. J Clin Invest. 2010; 120(6):1981–93. [PubMed: 20501942]
26. Faccio R, Novack DV, Zallone A, Ross FP, Teitelbaum SL. Dynamic changes in the osteoclast cytoskeleton in response to growth factors and cell attachment are controlled by beta3 integrin. J Cell Biol. 2003; 162(3):499–509. [PubMed: 12900398]
27. Mulari MT, Zhao H, Lakkakorpi PT, Vaananen HK. Osteoclast ruffled border has distinct subdomains for secretion and degraded matrix uptake. Traffic. 2003; 4(2):113–25. [PubMed: 12559037]
28. Blackshear PJ. The MARCKS family of cellular protein kinase C substrates. J Biol Chem. 1993; 268(3):1501–4. [PubMed: 8420923]
29. Coue M, Brenner SL, Spector I, Korn ED. Inhibition of actin polymerization by latrunculin A. FEBS Lett. 1987; 213(2):316–8. [PubMed: 3556584]
30. Hartwig JH, Thelen M, Rosen A, Janmey PA, Nairn AC, Aderem A. MARCKS is an actin filament crosslinking protein regulated by protein kinase C and calcium-calmodulin. Nature. 1992; 356(6370):618–22. [PubMed: 1560845]
31. van Meel E, Boonen M, Zhao H, Oorschot V, Ross FP, Kornfeld S, Klumperman J. Disruption of the Man-6-P targeting pathway in mice impairs osteoclast secretory lysosome biogenesis. Traffic. 2011; 12(7):912–24. [PubMed: 21466643]
32. Tu X, Joeng KS, Nakayama KI, Nakayama K, Rajagopal J, Carroll TJ, McMahon AP, Long F. Noncanonical Wnt signaling through G protein-linked PKCdelta activation promotes bone formation. Dev Cell. 2007; 12(1):113–27. [PubMed: 17199045]
33. Moonga BS, Stein LS, Kilb JM, Dempster DW. Effect of diacylglycerols on osteoclastic bone resorption. Calcif Tissue Int. 1996; 59(2):105–8. [PubMed: 8687978]
34. Trifaro JM, Gasman S, Gutierrez LM. Cytoskeletal control of vesicle transport and exocytosis in chromaffin cells. Acta Physiol (Oxf). 2008; 192(2):165–72. [PubMed: 18021329]
35. Pigeau GM, Kolic J, Ball BJ, Hoppa MB, Wang YW, Ruckle T, Woo M, Manning Fox JE, MacDonald PE. Insulin granule recruitment and exocytosis is dependent on p110gamma in insulinoma and human beta-cells. Diabetes. 2009; 58(9):2084–92. [PubMed: 19549714]
36. Kim J, Shishido T, Jiang X, Aderem A, McLaughlin S. Phosphorylation, high ionic strength, and calmodulin reverse the binding of MARCKS to phospholipid vesicles. J Biol Chem. 1994; 269(45):28214–9. [PubMed: 7961759]
37. Taniguchi H, Manenti S. Interaction of myristoylated alanine-rich protein kinase C substrate (MARCKS) with membrane phospholipids. J Biol Chem. 1993; 268(14):9960–3. [PubMed: 8486722]

38. Thelen M, Rosen A, Nairn AC, Aderem A. Regulation by phosphorylation of reversible association of a myristoylated protein kinase C substrate with the plasma membrane. Nature. 1991; 351(6324):320–2. [PubMed: 2034276]

39. Cuchillo-Ibanez I, Lejen T, Albillos A, Rose SD, Olivares R, Villarroya M, Garcia AG, Trifaro JM. Mitochondrial calcium sequestration and protein kinase C cooperate in the regulation of cortical F-actin disassembly and secretion in bovine chromaffin cells. J Physiol. 2004; 560(Pt 1): 63–76. [PubMed: 15133064]

40. Doreian BW, Fulop TG, Meklemburg RL, Smith CB. Cortical F-actin, the exocytic mode, and neuropeptide release in mouse chromaffin cells is regulated by myristoylated alanine-rich C-kinase substrate and myosin II. Mol Biol Cell. 2009; 20(13):3142–54. [PubMed: 19420137]

41. Vitale ML, Seward EP, Trifaro JM. Chromaffin cell cortical actin network dynamics control the size of the release-ready vesicle pool and the initial rate of exocytosis. Neuron. 1995; 14 (2):353–63. [PubMed: 7857644]

42. Rose SD, Lejen T, Zhang L, Trifaro JM. Chromaffin cell F-actin disassembly and potentiation of catecholamine release in response to protein kinase C activation by phorbol esters is mediated through myristoylated alanine-rich C kinase substrate phosphorylation. J Biol Chem. 2001; 276(39):36757–63. [PubMed: 11477066]

43. Burgoyne RD, Morgan A. Secretory granule exocytosis. Physiol Rev. 2003; 83(2):581–632. [PubMed: 12663867]

44. Brown AC, Oddos S, Dobbie IM, Alakoskela JM, Parton RM, Eissmann P, Neil MA, Dunsby C, French PM, Davis I, Davis DM. Remodelling of cortical actin where lytic granules dock at natural killer cell immune synapses revealed by super-resolution microscopy. PLoS Biol. 9(9):e1001152. [PubMed: 21931537]

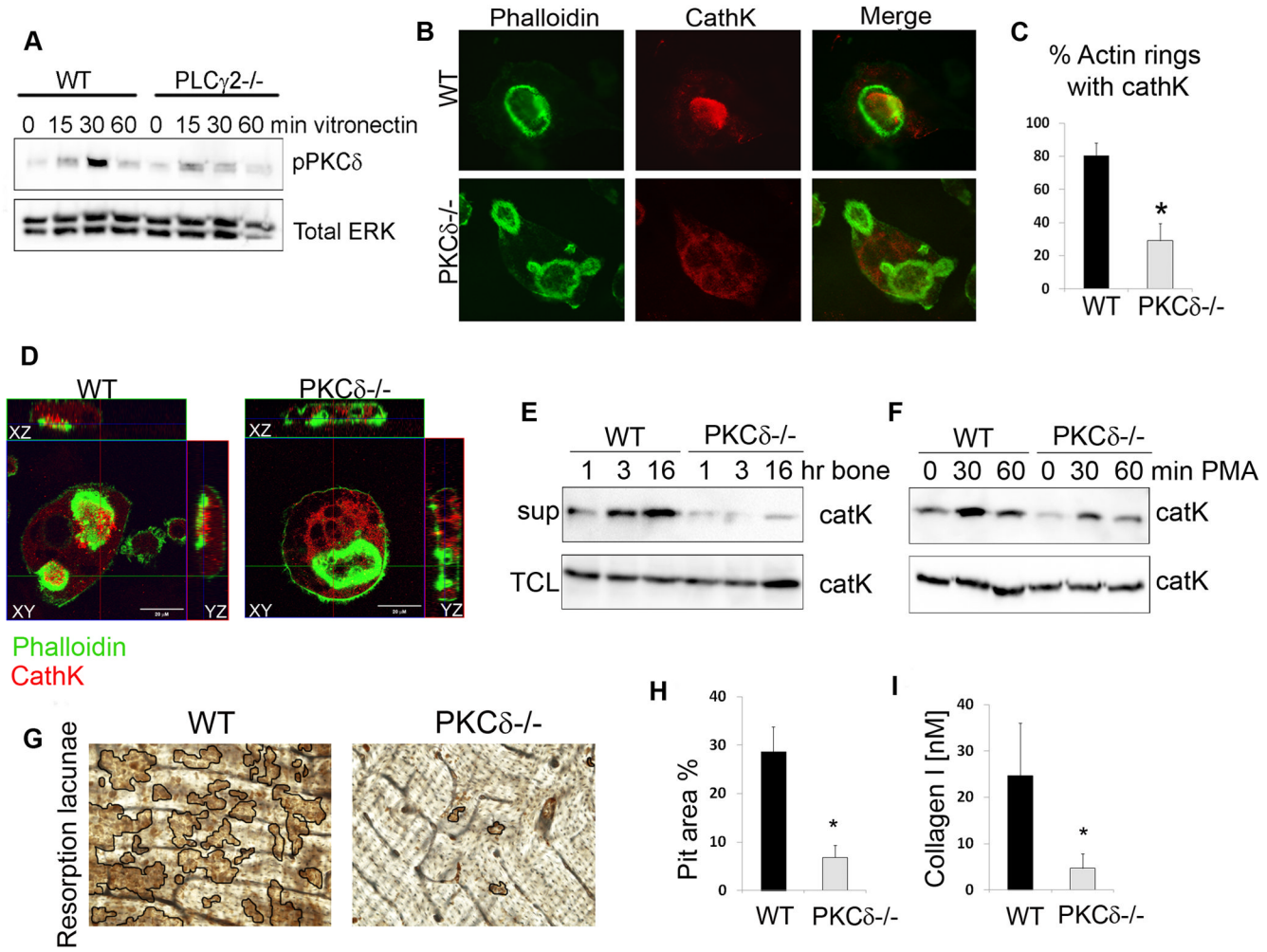

Figure 1. PKCδ is required for cathepsin K secretion

(A) WT and PLCγ2−/− pre-osteoclasts were stimulated by adhesion to vitronectin and phosphorylation of PKCδ was assessed in total cell lysates, using ERK as a loading control.

(B) WT and PKCδ−/− osteoclasts were grown on bone slices, fixed and stained with FITC-phalloidin (in green) and with a monoclonal antibody against cathepsin K (in red). Magnification 63X.

(C) Quantification of the percentage of actin rings with cathepsin K localized inside.

(D) Cells as in (B) were analyzed by confocal microscopy, and Z stack images were reconstructed using LSM software.

(E–F) WT and PKCδ−/− osteoclasts were stimulated with either bone particles (E) or PMA (F). Culture supernatant (sup) was collected and subjected to western blot analysis for the presence of cathepsin K. Cells in each well were lysed and served as total protein control (TCL).

(G) WT and PKCδ−/− osteoclasts were grown on bone slices for 10 days, cells were removed and resorption pits visualized by staining with peroxidase-conjugated wheat-germ agglutinin. Black lines delineate the resorbed areas.

(H) Area of bone resorption was determined using Image J software (n=5).

(I) Supernatant from cultures as in (G) was collected and analyzed for the presence of collagen type I fragment using a colorimetric Elisa method. Data are expressed as average +/− standard deviation. An asterisk (*) depicts differences with a p value <0.05.

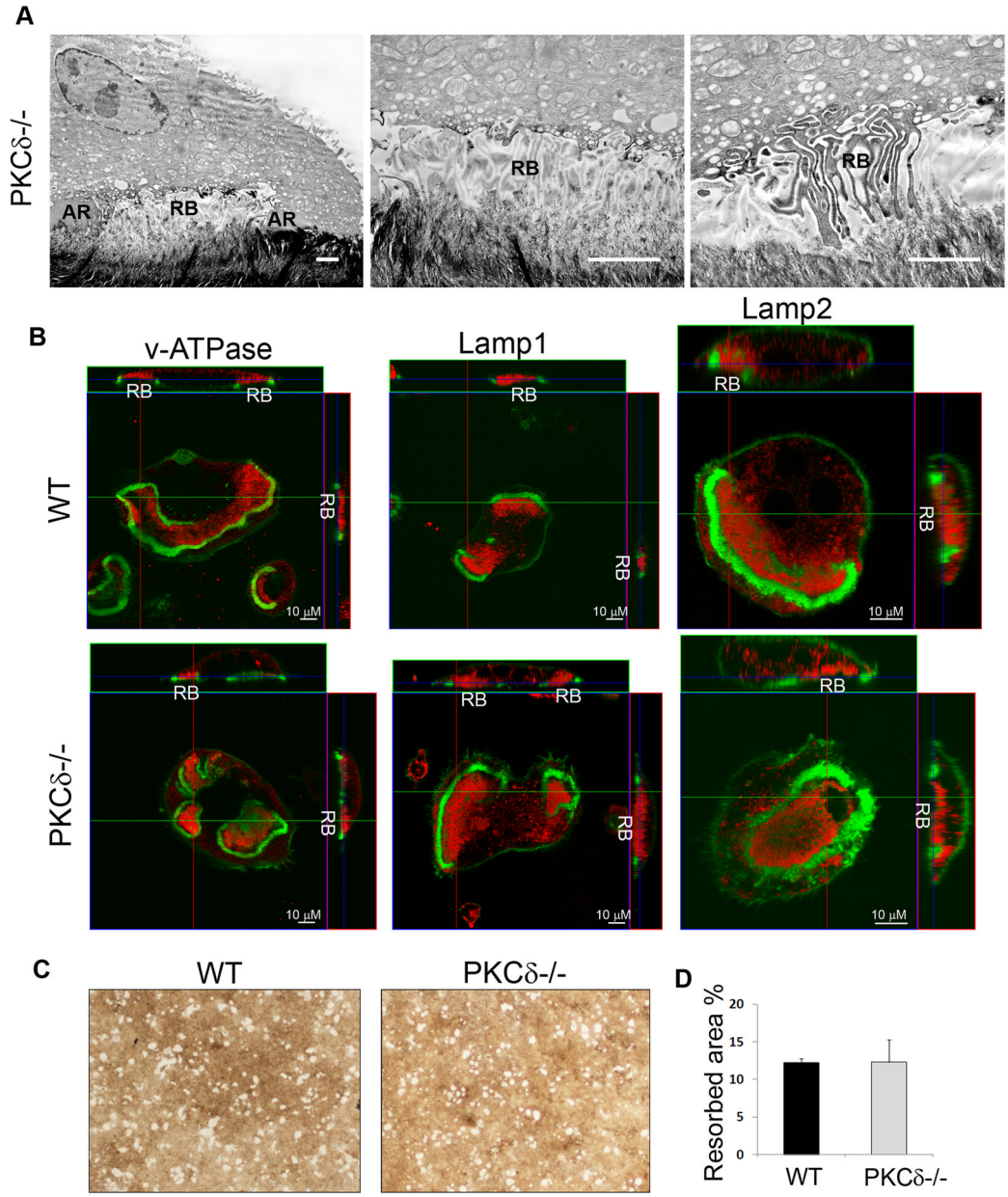

Figure 2. PKCδ-deficiency does not affect ruffled border formation or trafficking lysosomes containing the vATPase

(A) Transmission electron-microscopy was performed on PKCδ−/− osteoclasts plated on bone slices. Figures show actin rings (AR) and ruffled borders (RB). Scale bar 1 μm.

(B) WT and PKCδ−/− macrophages were grown on bone slices in osteoclastogenic medium for 10 days. Mature osteoclasts were fixed and stained with FITC-phalloidin (in green) and with antibodies against the subunit E of the v-ATPase, Lamp1 or Lamp2 (in red). Cells were analyzed by confocal microscopy, and Z stack images were reconstructed using LSM software. Magnification 63X.

(C–D) WT and PKCδ−/− macrophages were grown in the presence of M-CSF and RANKL on osteologic hydroxyapatite–coated slides for 4 days. Resorptive pits were visualized using a microscope without phase, magnification 20X, and quantified as percentage of resorbed area. Data are expressed as average +/− standard deviation.

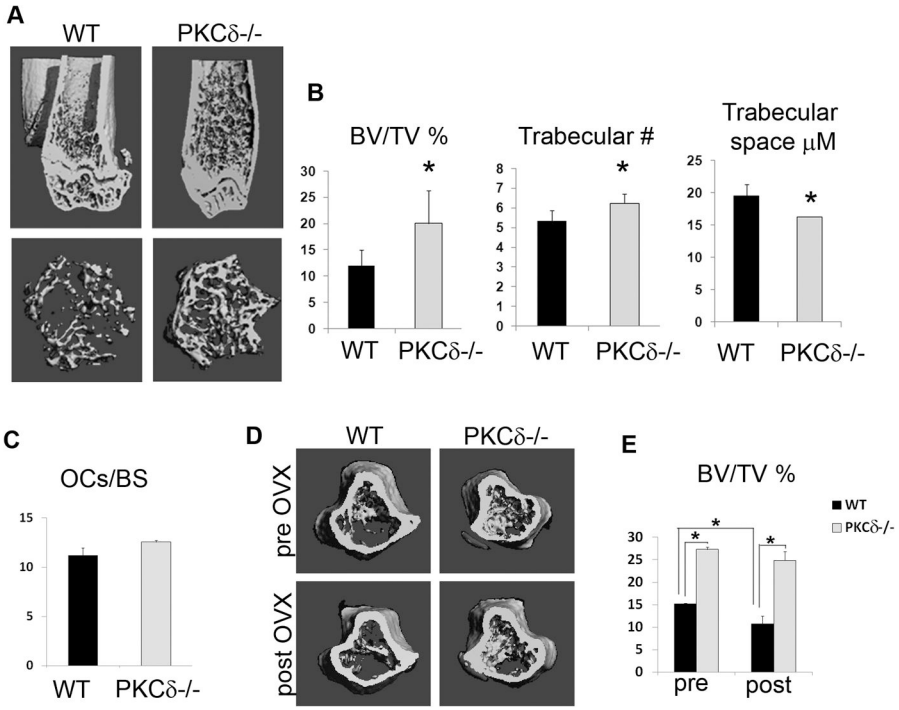

Figure 3. PKCδ regulates bone homeostasis in physiological and pathological conditions

(A) Femurs of 8 week-old WT and PKCδ−/− mice were subjected to μCT analysis to detect trabecular bone. Images show representative 3D reconstructions.

(B) Quantitative analysis of bone parameters were obtained from μCT data. Data are expressed as average +/− standard deviation. An asterisk (*) depicts differences with a p <0.05.

(C) Histomorphometric analysis of the number of osteoclasts per bone surface from sections of 8 week-old mice (n=4/group).

(D) WT and PKCδ−/− female mice were subjected to ovariectomy and trabecular bone volume versus total bone volume (BV/TV) was determined using vital μCT analysis before (pre OVX) and 1 month after ovariectomy (post OVX). Images show representative 3D reconstructions.

(E) Quantitative analysis of percent trabecular bone volume versus total bone volume (n=4/group). An asterisk (*) depicts differences with a p value <0.05.

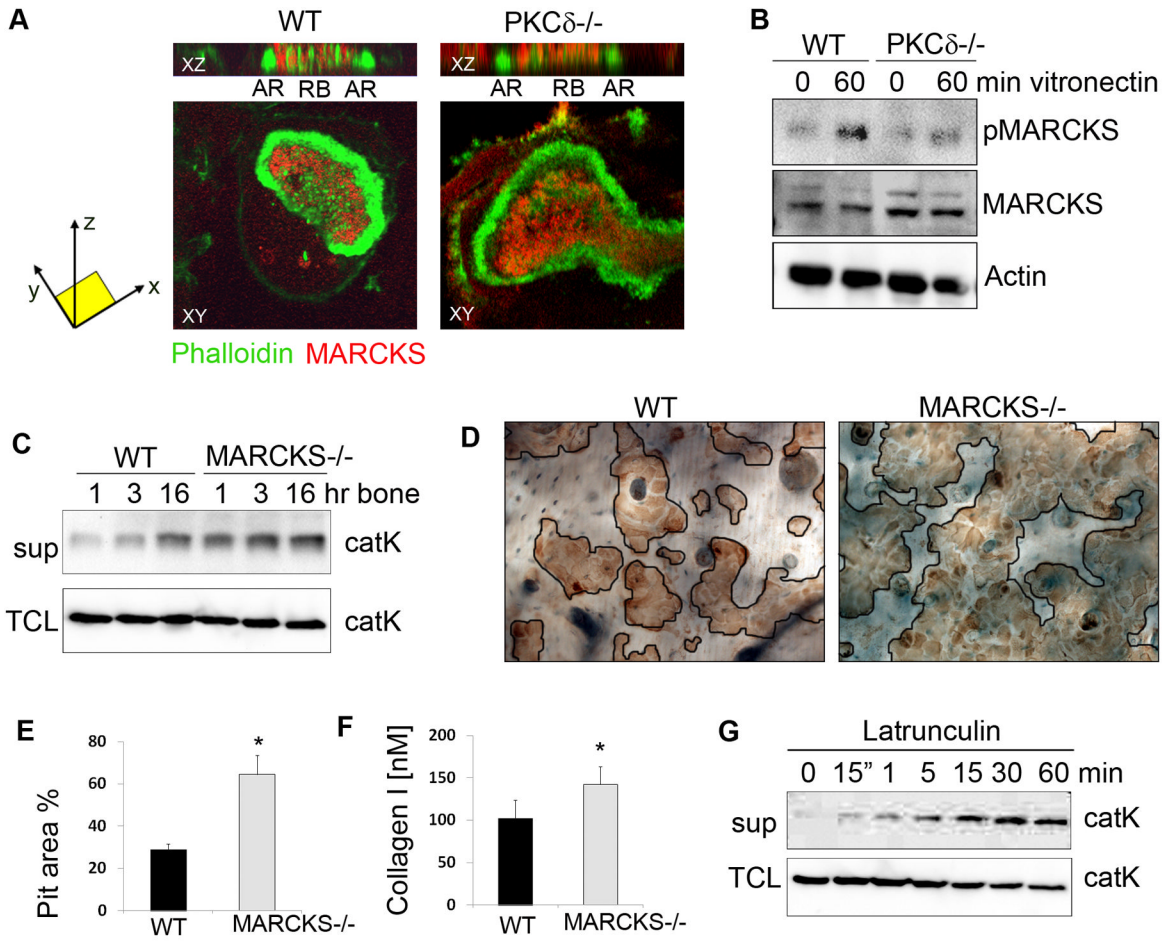

Figure 4. MARCKS regulates cathepsin K secretion downstream of PKCδ

(A) WT and PKCδ−/− osteoclasts were grown on bone slices, fixed and stained with FITC-phalloidin (in green) and with a monoclonal antibody against MARCKS (in red). Cells were analyzed by confocal microscopy and Z stack images were reconstructed using LSM software (AR=actin ring; RB=ruffled border).

(B) WT and PKCδ−/− pre-osteoclasts were stimulated by adhesion to vitronectin. Cells were lysed and equal amounts of total cell lysates were western blotted for the indicated proteins. Actin served as a loading control.

(C) WT and MARCKS−/− osteoclasts were stimulated for the indicated times with bone particles, and culture medium supernatant (sup) was analyzed for the presence of cathepsin K. Cells in each well were lysed and served as total protein control (TCL).

(D) WT and MARCKS−/− osteoclasts were grown on bone slices for 10 days, cells were removed, and resorption pits visualized by staining with peroxidase-conjugated wheat-germ agglutinin. Black lines delineate the resorbed areas.

(E) Area of bone resorption per field was determined using Image J software.

(F) Supernatant medium from culture as in (D) was analyzed for the presence of collagen type I fragments using a colorimetric Elisa method. Data are expressed as average +/− standard deviation. An asterisk (*) depicts differences with a p value <0.05.

(G) WT osteoclasts were treated with Latrunculin A and medium supernatant (sup) was collected and subjected to western blot for cathepsin K. Cells in the well were lysed as a total protein control (TCL).

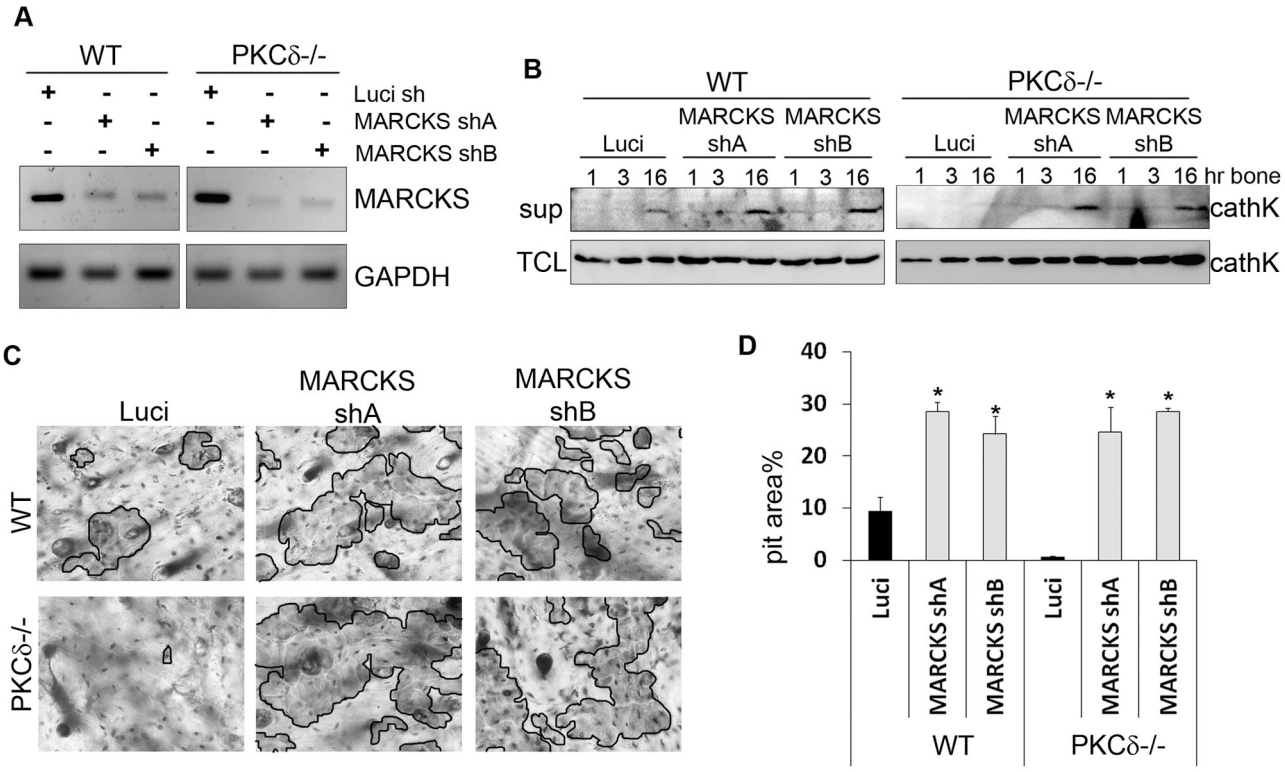

Figure 5. MARCKS silencing in PKCδ−/− osteoclasts rescues cathepsin K lysosome exocytosis

(A) WT and PKCδ−/− macrophages were lentivirally transduced with two different MARCKS silencing constructs or with shRNA directed towards Luciferase as a negative control. Efficiency of MARCKS knock-down was determined using semi quantitative RT-PCR. GAPDH served as a loading control.

(B) Cells as in (A) were cultured in osteoclastogenic medium for 7 days and stimulated for different time points with bone particles. Medium supernatant (sup) was collected and subjected to western blot analysis for the presence of cathepsin K. Cells in the well were lysed as a total protein control (TCL).

(C) Cells as in (A) were grown on bone slices in osteoclastogenic medium for 10 days. Cells were then removed and resorption pits visualized by staining with peroxidase-conjugated wheat-germ agglutinin. Black lines delineate the resorbed areas.

(D) Area of bone resorption per field was determined using Image J software and graphed for each sample. Data are expressed as average +/− standard deviation. An asterisk (*) depicts differences with a $p < 0.05$.

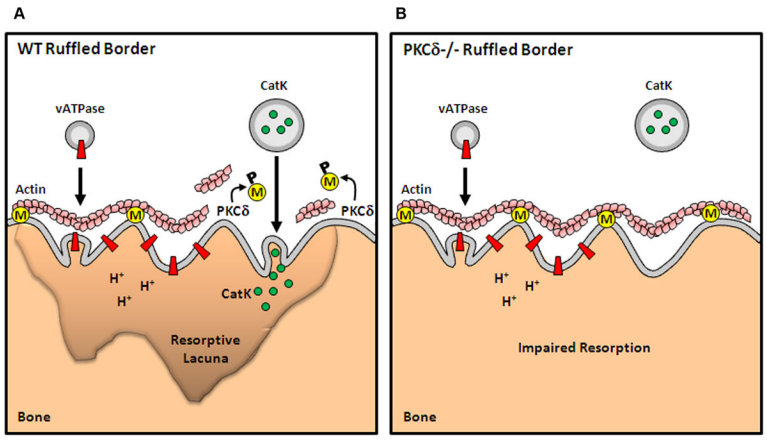

Figure 6. Specific regulation of cathepsin K lysosomal secretion by PKCδ and MARCKS

(A) MARCKS (**M**, in yellow) binds to actin and tethers filaments to the plasma membrane of the ruffled border. PKCδ-mediated phosphorylation (**P**) of MARCKS displaces MARCKS from the membrane and impairs its actin-binding capacity. MARCKS displacement produces a local release of actin filaments, thus allowing cathepsin K vesicle secretion.

(B) In absence of PKCδ, MARCKS is stabilized at the membrane. While failure to disrupt the actin barrier does not affect ruffled border formation or translocation of vesicles containing the v-ATPase, it impairs cathepsin K release, thus inhibiting the cell resorptive ability.